Origins of Delays in Monolayer Kinetics: Phospholipase A_2 Paradigm†

Yolanda Cajal,*,‡ Otto G. Berg,§ and Mahendra Kumar Jain⊥

Departament de Fisicoquimica, Facultat de Farmacia, Universitat de Barcelona, Barcelona 08028, Spain, Department of Molecular Evolution, Uppsala University Evolutionary Biology Centre, Uppsala, Sweden, and Department of Chemistry and Biochemistry, University of Delaware, Newark, Delaware 19716

Received January 26, 2004; Revised Manuscript Received April 7, 2004

ABSTRACT: The interfacial kinetic paradigm is adopted to model the kinetic behavior of pig pancreatic phospholipase A_2 (PLA2) at the monolayer interface. A short delay of about a minute to the onset of the steady state is observed under all monolayer reaction progress conditions, including the PLA2-catalyzed hydrolysis of didecanoylphosphatidyl-choline (PC10) and -glycerol (PG10) monolayers as analyzed in this paper. This delay is independent of enzyme concentration and surface pressure and is attributed to the equilibration time by stationary diffusion of the enzyme added to the stirred subphase to the monolayer through the intervening unstirred aqueous layer. The longer delays of up to several hours, seen with the PC10 monolayers at >15 mN/m, are influenced by surface pressure as well as enzyme concentration. Virtually all features of the monolayer reaction progress are consistent with the assumption that the product accumulates in the substrate monolayer, although the products alone do not spread as a compressible monolayer. These results rule out models that invoke slow "activation" of PLA2 on the monolayer. The observed steady-state rate on monolayers after the delays is <1% of the rate observed with micellar or vesicles substrates of comparable substrate. Together these results suggest that the monolayer steady-state rate includes contributions from steps other than those of the interfacial turnover cycle. Additional considerations that provide understanding of the pre-steady-state behaviors and other nonideal effects at the surface are also discussed.

The interfacial kinetic paradigm for phospholipase A_2 (PLA2[1]) bound to micellar and bilayer interfaces of phospholipid is well established (*1*, *2*). In the presence of anionic charge at the interface, PLA2 shows a highly processive interfacial turnover due to tight binding of the enzyme and k_{cat}* activation. In these well-defined systems, the primary rates and equilibrium constants for the interfacial catalysis have been quantitatively obtained. The analysis has also provided insights into the theoretical and technical limitations of the kinetic assays with low enzyme processivity, such as on the zwitterionic interfaces. Additional limitations are predicted for the monolayer system (*2*). Due to its apparent simplicity, the study of interfacial enzyme kinetics at the air−water interface has attracted considerable attention (*3*−*15*). For a variety of reasons, developed below and discussed elsewhere (*1*, *2*, *16*, *17*), monolayer assays have provided few insights into the primary events of the interfacial turnover. Typically, monolayer reaction progress shows anomalous delays to the steady state where the rates are <1% of the rates observed at other interfaces. Also considerable evidence has accumulated against the simplifying assumptions necessary for the interpretation of the monolayer kinetics (*17*−*23*).

Interpretations of the monolayer kinetics in the published literature (*3*−*15*) are based on a grail of assumptions that are not valid for the identification of the reaction path or the microscopic steady-state condition for the turnover (*1*, *2*). As shown and developed in this paper and outlined below, kinetic analysis of the monolayer reaction progress is not possible. For an appreciation of the basic arguments behind this assertion, in this paper, we critically analyze key features of reaction progress in terms of a minimal model shown in Figure 1. Operationally, the E to E* step for the binding of the enzyme to the substrate monolayer is followed by the processive turnover by E* through the interfacial Michaelis−Menten turnover path. Analysis of the interfacial turnover path is straightforward if the turnover processivity is virtually infinite (*1*, *2*, *24*, *25*), that is, if E* does not leave the interface and if the substrate replenishment for the turnover is rapid on the scale of the turnover time.

If the residence time of E* cannot be defined, it is not trivial to establish either the E to E* binding equilibrium at the monolayer or the kinetic contributions of the forward and reverse steps. Additional complications come into play if the product release or substrate replenishment cannot be considered instantaneous. Thus the amounts of both enzyme

† This work was supported by grants from Ministerio de Ciencia y Tecnología-FEDER, (Grant SAF2002-01740 to Y.C.) and Swedish Research Council (to O.G.B) and Grant PHS-GM29703 (to M.K.J.).

* Corresponding author: phone 34-3-4035988; fax 34-3-4035987; e-mail ycajal@ub.edu.

‡ University of Barcelona.

§ Uppsala University.

⊥ University of Delaware.

[1] Abbreviations: FA, decanoic acid; LPC, 1-decanoylphosphatidylcholine; PC10, 1,2-didecanoylphosphatidylcholine; PG10, 1,2-didecanoylphosphatidylglycerol; PLA2, group IB phopholipase A_2 from pig pancreas; products, the equimolar mixture of the products of hydrolysis of PC10 by PLA2, LPC + FA (1:1). The model and associated constants are defined in Figure 1. The enzyme kinetic parameters have their standard significance except that the catalytic turnover occurs only at the interface (*1*, *2*).

10.1021/bi049816t CCC: $27.50
Published on Web 06/19/2004

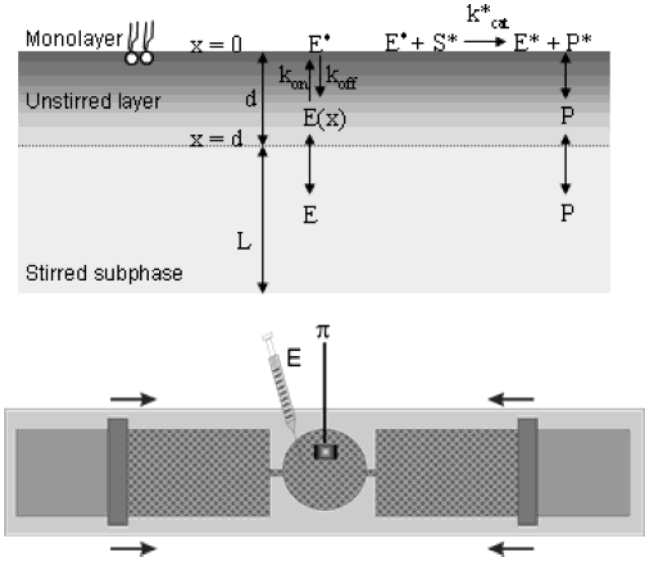

FIGURE 1: The upper panel shows a cross-section to emphasize the microscopic features in the vicinity of the phospholipid headgroups at the air−water monolayer interface. Note that the stirred bulk aqueous subphase is separated from the headgroup region by an unstirred layer (shaded) of the aqueous phase. Before encountering the interface, the enzyme E in the bulk aqueous phase diffuses through the unstirred layer. E* at the interface mediates the processive interfacial turnover on S*, the substrate in the interface. Not all the product released in the interface (P*) leaves the interface. The lower panel shows the top-down view of the three-compartment trough used for the zero-order kinetic measurements. The schematics are not drawn to scale.

and product bound in the monolayer can change during the experiment, and the assay does not provide any direct means of determining these amounts. Without this information, it is impossible to determine the primary catalytic parameters for the interfacial turnover. Experimental evidence in this paper also shows that certain assumptions made in the earlier interpretations of monolayer kinetics are not valid. For example, the product desorption from the monolayer is not rapid, and the interfacial turnover is not the rate-limiting step.

Some of the features of the monolayer reaction progress (*3*−*17*) are not observed during the reaction progress with micellar and bilayer dispersions (*1*, *2*, *26*−*28*). With a focus on such differences, the present study is designed to address issues unique to the monolayer assays such as the trough geometry and the interface area in contact with the unstirred layer. As developed in ref *2*, the monolayer reaction progress can be modeled if we know the parameters for the equilibration and exchange of the enzyme, as well as substrate and products, between the interface and the stirred bulk aqueous phase through the intervening unstirred aqueous layer (Figure 1). The equilibration by stationary diffusion through the unstirred aqueous layer occurs on the time scale of about a minute. The pressure-dependent longer delays seen only with the zwitterionic PC10 monolayer, but not with the anionic PG10 monolayer, are attributed to the product accumulation that influences the E to E* equilibrium and the k_{cat}* activation as seen in bilayers and micelles (*1*, *2*, *26*−*30*).

EXPERIMENTAL PROCEDURES

PC10, PG10, and LPC10 were from Avanti (Alabaster, AL). FA (decanoic acid) was from Aldrich. PLA2 was purified as before (*24*, *25*). Other reagents were analytical grade. Chloroform (HPLC grade, Fisher Scientific) was used as the monolayer spreading solvent for all lipids. Buffers were made in double-distilled and deionized (Milli-Q system, Millipore Corp.) water.

Monolayer Preparation and Kinetic Protocols. All measurements were carried out at room temperature, 24 °C, under the zero-order kinetic conditions. The progress curves were recorded on a computer-controlled monolayer system, KSV5000 (KSV, Helsinki, Finland). To avoid carryover of lipid and protein, the PTFE (Teflon) trough and the Wilhelmy plate were thoroughly cleaned with hot double-distilled water at >75 °C.

Figure 1 (bottom) shows the three-compartment zero-order Langmuir trough used for the kinetic experiments. The central cylindrical reaction compartment (7 cm diameter) is connected through narrow channels (3 mm width and less than 1 mm depth) of etched glass to two rectangular substrate reservoir compartments (width 7.5 cm, length 21.5 cm). A sand-blasted platinum plate connected to an electrobalance was set up in the reaction compartment for continuous monitoring of the surface pressure. With the movable Teflon barrier placed at the outer extreme of each reservoir compartment, the three compartments were filled with 10 mM Tris and 2 mM $CaCl_2$ at pH 8.0 (200 mL + 40 mL + 200 mL) in such a way that the buffer is connected through the channels and a meniscus of 2−3 mm is formed on the barriers. Before spreading the substrate, the barriers were moved close to the channels and the surface was cleaned to $\pi = 0$ by vacuum suction before returning the barriers to their original position. The surface-active impurities from the surface were removed in this manner by repeating the procedure three times. With barriers in the extreme positions, phospholipid monolayer was spread on the surface by adding 1−3 μL drops of the stock solution in chloroform. Typically, a total of 30−60 μL of 2 mM stock solution was spread to achieve the desired surface pressure. If necessary, excess phospholipid was removed or the monolayer compressed to the desired pressure.

With the surface pressure stable (for at least 5 min) at a constant preset value, a known aliquot of PLA_2 was injected with a microsyringe into the stirred aqueous subphase of the reaction compartment. The surface pressure decreases as the substrate is hydrolyzed and some of the product begins to leave the monolayer in the reaction compartment. During the zero-order reaction progress, the surface pressure is kept constant at the preset value through the electronic feedback that moves the barriers in the reservoir compartments such that the monolayer in the reaction compartment is replenished. Monolayer from the reservoir compartment diffuses into the reaction compartment through narrow surface channels, typically with a lag of less than 10 s. Thus the rate of reduction of surface area in the reservoir compartment ($mm^2 \cdot min^{-1}$) is proportional to the amount of product that leaves the monolayer. The slope of the reaction progress curve as a function of time (derivative in $mm \cdot min^{-1}$) was calculated from the average barrier displacement over an interval of 40 s. Such computer-generated measures of the rate as a function of time are able to continuously track and differentiate modest changes in the slope with time. The time to reach half of the maximum peak in the derivative plot provides an objective measure of the delay to the steady state, and it is also more reliable than the extrapolation of the

steady-state rate to the *x*-axis of a chart record. It is quite likely that the some of the difficulties encountered in the earlier studies were the result of manual processing of the reaction progress curve to obtain the rate and the lag period by extrapolation of the maximum slope to the time axis.

To estimate the turnover rate, it is often assumed that all the product molecules rapidly leave the monolayer. In terms of all the preceding assumptions, the slope is related to the number of substrate molecules hydrolyzed per minute per molecule of enzyme (s^{-1}) added to the aqueous phase. The area per substrate molecule at the experimental surface pressure is obtained from the number density in the surface pressure−area isotherms. Monolayer properties at constant area were also monitored as an increase in the surface pressure using a single cylindrical Teflon trough (7 cm diameter or 38.5 cm^2 area) containing stirred 40 mL aqueous phase with 10 mM Tris and 2 mM $CaCl_2$ at pH 8.0. Increasing amounts of the desired phospholipid or the products of hydrolysis were added from a 2 mM lipid stock solution in chloroform while the surface pressure was continuously recorded.

RESULTS

Constraints of Monolayer Kinetics. Key features of the monolayer trough geometry that influence the reaction progress are shown in Figure 1. The aqueous phase is stirred, but there remains an unstirred layer of effective thickness *d* just below the monolayer. Besides the turnover parameters, it is necessary to consider not only the rate and equilibria that control the steady-state levels of the enzyme at the interface but also the rate and equilibria for the distribution and partitioning of the substrate and products between the monolayer and the aqueous phase including the walls of the trough.

Primary variables that control the rate of the product formation are the amounts of the substrate, enzyme, and product in the monolayer. Our analysis shows that at least two other processes are at work before the onset of the steady state. A short delay of about a minute to the steady state is seen in all cases. It can be attributed to the stationary diffusion of PLA2 from the bulk aqueous phase to the interface through the unstirred layer (cf. Figure 1 and eq 1). A longer delay is observed under certain conditions with PC10 monolayer, but not with PG10. It is attributed to the development of the anionic charge at the interface by the product accumulation and the consequent increase in the binding of PLA2 to the interface, its k^*_{cat} activation or both.

Pre-Steady-State Delays. The time course of the zero-order reaction progress for the PLA2-catalyzed hydrolysis of PC10 monolayer at two different pressures is compared in Figure 2. The derivative plot (slope) gives the rate at 40 s intervals. Here the delay is defined as the time to reach half of the steady-state (maximum) rate. This value is comparable to that obtained by the extrapolation of the steady-state part of the reaction progress to the *x*-axis.

Three features of the derivative plot in Figure 2 are noteworthy. First, at high surface pressure, the onset of the increase in the rate is complex, and certainly, it is not exponential. An exponential time course is expected if the binding of the enzyme from the aqueous phase to the interface were dominated by a single intrinsic rate constant

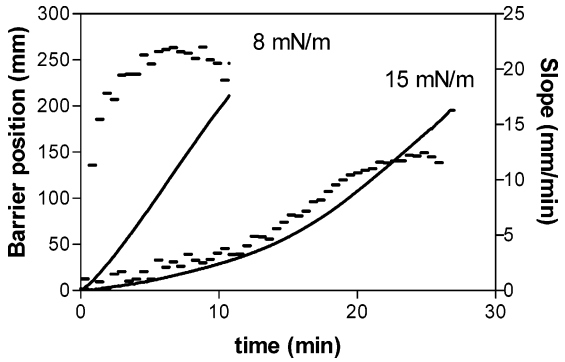

FIGURE 2: Reaction progress for the hydrolysis of PC10 monolayer at 8 or 15 mN/m by 10.6 μg of PLA2. Continuous line tracks the change in the position of the barrier (mm). The steps (broken line in units of mm/min) at 40 s intervals are for the derivative of the progress curve to give the slope at the intervals of 40 s. Unless noted, here and in all other measurements, the 40 mL of aqueous subphase in the reaction compartment is 10 mM Tris and 2 mM $CaCl_2$ at pH 8.0. The amount of PC10 in the reaction compartment of monolayer area of 38.5 cm^2 is about 9.17 nmol at 15 mN/m. A somewhat lower value of the phospholipid at the surface is estimated from the pressure−area curves where the area per molecule is 77 $Å^2$ at 15 mN/m., that is, the amount of lipid on 38.5 cm^2 surface is 8.3 nmol.

for the "interfacial activation" or "penetrating power" (*3*−*10*). Second, the dependence of the delay on the surface pressure of PC10 monolayer is not observed with PG10 monolayer as described later. Third, the maximum rate at the end of the delay begins to decrease slowly, which suggests that the substrate mole fraction in the monolayer decreases even though the surface pressure remains constant.

Therefore, a short delay of 1−2 min to the steady state, as also noted in virtually all the published monolayer kinetic measurements, is unlikely to be related to the catalytic properties of PLA2. Not only is this short delay observed in the monolayer reaction progress with virtually all the interfacial enzymes, but also such a delay is not observed with the micellar and vesicle interfaces. As developed and simulated later (eq 1), a delay of 1−2 min is predicted for the stationary diffusion of PLA2 through an unstirred layer of ca. 0.001 cm.

Dependence of the Delay on the Enzyme Concentration. There are two major difficulties in the interpretation of the progress of a reaction of hydrolysis on monolayers. First, it is not possible to measure the thickness of the unstirred layer through which the enzyme added to the aqueous phase diffuses to the interface. Second, the exact amounts of product and enzyme in the monolayer cannot be directly measured. Therefore such contributions can only be indirectly evaluated. Results in Figure 3 show a nonlinear dependence of the delay and rate on the total enzyme concentration. For the PC10 monolayer at 8 mN/m at all PLA2 concentrations, the delay is about 1 min. At the higher surface pressures, the delay is longer, that is, up to 70 min depending on the enzyme concentration and the surface pressure, as shown in Figure 3A. The long delay time decreases with increasing enzyme concentration. This is expected if the long delay observed at the higher surface pressures is related to a change in the PC10 monolayer induced by the enzyme action. There is another unusual feature of the effect of the enzyme concentration on the steady-state rate (Figure 3B): the rate does not change significantly with the surface pressure, and

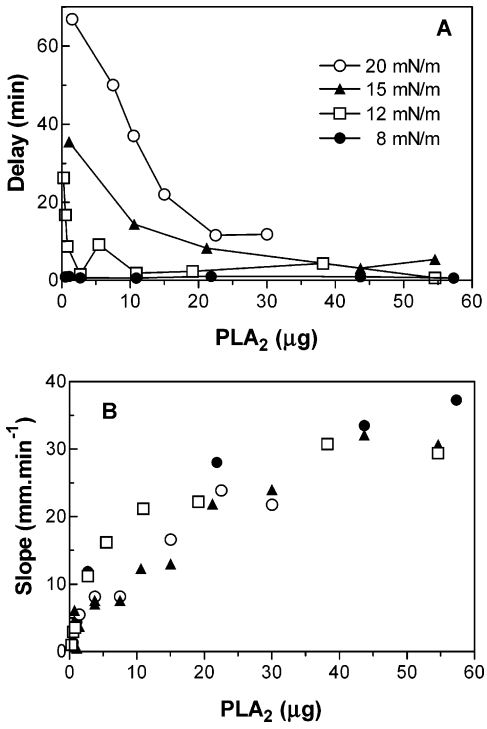

FIGURE 3: The PLA2 concentration dependence of (A) the delay and (B) the maximum slope at the steady state in the zero-order reaction progress for the hydrolysis of a PC10 monolayer at constant pressure (mN/m): (○) 20, (▲) 15, (□) 12, and (●) 8. Other conditions were as described in Figure 2.

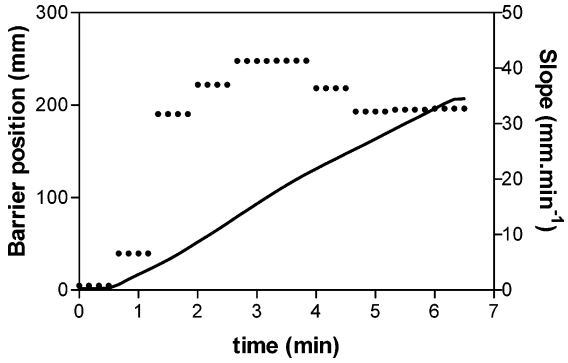

FIGURE 4: Reaction progress (continuous line) and steady-state rate (slopes, dotted line) for the hydrolysis of PG10 monolayer at 20 mN/m by 10.5 μg of PLA2.

at all surface pressures, it saturates at the higher enzyme concentrations. Together, the results in Figures 2 and 3 are inconsistent with all variations on the theme of intrinsically slow "penetration or activation" of PLA2 at the substrate monolayer.

Only the Short Delay Is Observed with Monolayer of Anionic PG10. Compared to a delay of more than 30 min with the PC10 monolayer at 20 mN/m (Figure 3), for the same amount of enzyme only a short delay of about a minute is observed with PG10 monolayer at 20 mN/m (Figure 4). In both cases, the peak rate decreases at the longer times beyond the onset of the steady state. Long delay of >2 min is not observed with PG10 monolayers under the range of conditions that we have studied. For example, as shown in Figure 5A, the delay remains constant at less than 1 min as the peak rate increases modestly up to a pressure of 28 mN/m. Also, at 20 mN/m, the delay of about 1 min is independent of the enzyme concentration (Figure 5B). These results show

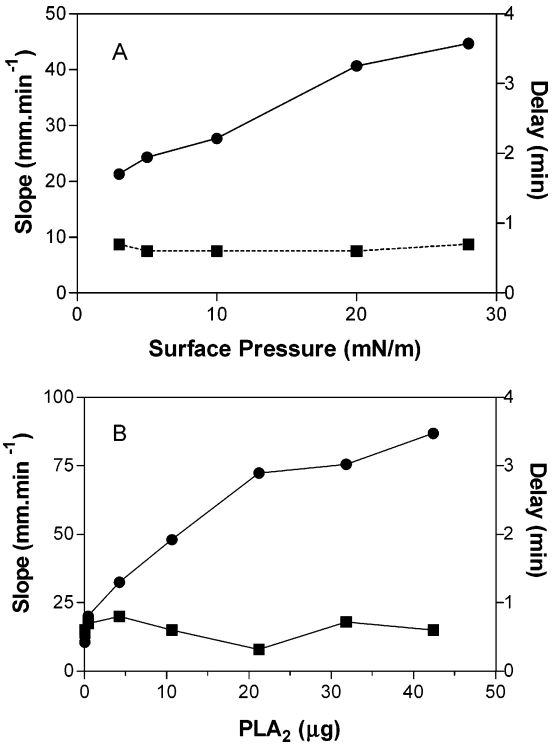

FIGURE 5: Surface pressure dependence (A) of the (■) delay and (●) maximum slope for the hydrolysis of PG10 by 10.5 μg of PLA2 and PLA2-concentration dependence (B) of the delay (■) and the maximum slope (●) for the hydrolysis of PG10 at 20 mN/m. Other conditions were as described in Figure 2.

that only the short delay is seen during the hydrolysis of PG10 monolayer at all surface pressures. In analogy with the difference between the interfacial kinetic behavior of the anionic versus the zwitterionic micelles and bilayers (*1*, *2*, *20*−*25*), we attribute the difference to the changes in PLA2 induced by the interfacial anionic charge.

The Long Delay Decreases in the Presence of the Products or NaCl. The long delay observed with the zwitterionic PC10 monolayer can be attributed to the time needed to accumulate a minimum amount of anionic charge due to the products of hydrolysis. For example, as shown in Figure 6A, the long delay of over 90 min at 23 mN/m diminishes to less than 3 min if the reaction progress is monitored with monolayer spread on 4 M NaCl due to the preferential adsorption of anionic chloride into micellar or bilayer interface of zwitterionic phosphatidylcholine (*25*). The long delay of over 100 min (not shown) under these conditions decreases if the products of hydrolysis are added to the PC10 monolayer before initiating the reaction progress (Figure 6B): the delay is 26 min with 12 mol % product and 5 min with 66 mol % product. As also shown in Figure 6B, the delay is less than 3 min if the PC10 monolayer is spread on the subphase containing PLA2 and the hydrolysis products of PC10 from the previous run at the same surface pressure. Together, these results show that the long delay during the PC10 monolayer reaction progress at constant pressure decreases in the presence of the added products of hydrolysis.

Observed Monolayer Rates Are Exceedingly Slow. Results in Figures 3B and 5B show that for both substrates the observed steady-state rates (slope) saturate with the amount of enzyme added to the subphase. Also for both substrates, irrespective of the enzyme concentration or the surface

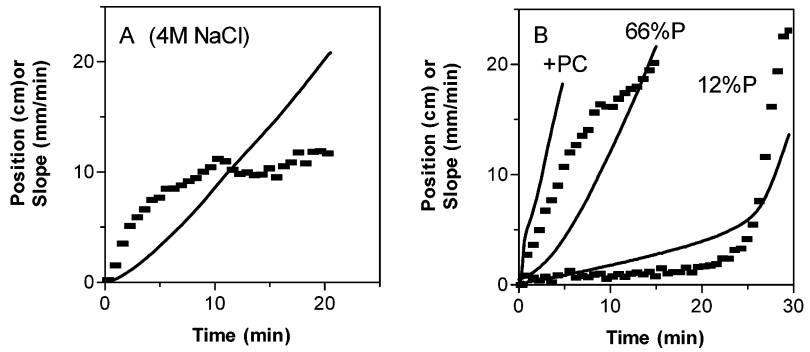

FIGURE 6: Reaction progress for the hydrolysis of PC10 monolayer at 23 mN/m by 10.9 μg of PLA2 (in all cases) (A) with 4 M NaCl in the aqueous subphase or (B) with 12 or 66 mol % of product added to the monolayer before initiating the reaction progress. Panel B also shows the reaction progress (+PC, without the derivative plot) on a second aliquot of PC10 spread on the subphase after the complete hydrolysis of the first aliquot of the same amount of PC10 that showed a long delay of over 100 min. Other conditions and controls are as described in Figure 2.

Table 1: The Apparent Maximum Rate of Hydrolysis (s^{-1}) of PC10 and PG10 by PLA2

conditions	PC10	PG10
monolayer[a]	0.04	0.2
vesicles[b]	400	560

[a] Rates for 10 μg of PLA2 in the subphase were obtained from the steady-state slope in the reaction progress (Figures 3B and 5B). The number density of the substrate molecules was used to convert the area change to turnover number on the basis of the total enzyme added to the subphase (*5*). [b] The turnover rate of hydrolysis of the aqueous dispersions were obtained by pH state titration at the bulk saturating amounts of the substrate (*25*, *30*, *31*).

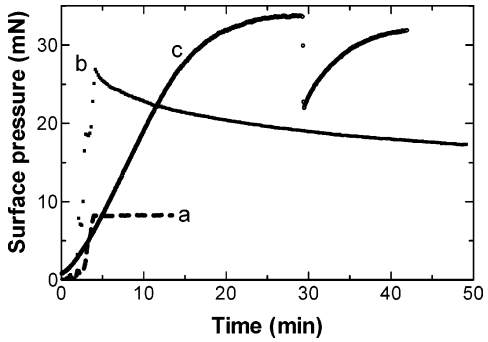

FIGURE 7: The time course of the change in the surface pressure in a single compartment trough after the addition of PG10 to 40 mL of stirred aqueous subphase with 38.5 cm^2 surface area: (a) 0.0088 or (b) 0.012 μmol of PG10 spread onto the surface. For line c, 0.05 μmol of PG10 was added into the aqueous subphase, and then at 30 min, the surface monolayer was partially removed by aspiration.

pressure, the apparent monolayer rate at the steady state is exceedingly low. As summarized in Table 1, with 10 μg of PLA2 in the subphase the apparent monolayer rate is 0.04 s^{-1} for PC10 and about 0.2 s^{-1} for PG10, which are less than 0.1% of 400−500 s^{-1} measured at the saturating concentrations of the micellar aqueous dispersions of PC10 or PG10. Based on the interfacial kinetic paradigm (Figure 1), there are at least three types of effects that could lead to the apparently lower observed monolayer rates calculated from the rate of barrier displacement. The intrinsic catalytic turnover rate at the monolayer interface is unlikely to be significantly different from that at the micellar or bilayer interfaces. Note that the chain length of the substrate has at best a modest effect (less than 3-fold) on the observed turnover rate at the micellar or bilayer organization (*25*, *30*, *31*) with internal surface pressure of about 30 mN/m. A 1000-fold difference between the monolayer and micellar rates (Table 1) is therefore likely to be due to the fraction of the total enzyme bound to the monolayer and the turnover efficiency of the bound enzyme. In addition, a slow product desorption rate from the monolayer could change not only the surface charge on the monolayer but also the steady-state mole fraction of the substrate and product.

There are no satisfactory methods available for determining the dissociation constant, K_d, or the amount of E* on the monolayer. Therefore the fraction of PLA2 bound to monolayer can only be guesstimated. Based on the micellar substrate concentration dependence of the enzyme kinetics, the apparent K_d is in the range of 10^{-4} M (*31*). Based on the total PC10 or PG10 concentration, [M*], of 0.25 μM (0.01 μmol in 40 mL of subphase in the reaction compartment), the ratio of the free/bound enzyme, $E_F/E^* = K_d/[M^*]$, would be about 400. This estimate is somewhat larger than the experimental estimate that 1−5% of radiolabeled PLA2 binds to the monolayer (*8*). The effects of the interfacial anionic charges and the product accumulation in the monolayer are discussed further below. Beyond this, the possibility that a significant fraction of E_F in the aqueous subphase is irreversibly adsorbed on the surface of the Teflon trough can be ruled out on the basis of the results that a fresh PC10 monolayer spread on the surface of a hydrolyzed monolayer does not show the long delay (*17*). Such a loss of the long delay for the first-order reaction progress would be seen only if both E_F and products redistribute in the freshly spread PC10 monolayer within the duration of the short delay. Note that the products of hydrolysis from a fully hydrolyzed PC10 monolayer do not form a compressible monolayer (*17*).

Equilibration of PG10 and PC10 at the Monolayer Interface. The calculation of the catalytic turnover rate from the speed of barrier displacement is based on the assumption that the product formed in the monolayer rapidly and completely leaves the interface on the time scale of the turnover and also that all the substrate is present only in the monolayer. Under the zero-order kinetic conditions, this means that the product is rapidly replaced with an equivalent amount of substrate only from the reservoir compartment. Results described below show that these assumptions are not valid. As shown in Figures 7 and 8 at least some of the phospholipid at the higher surface pressure remains in the aqueous phase, and the rate at which phospholipid partitions

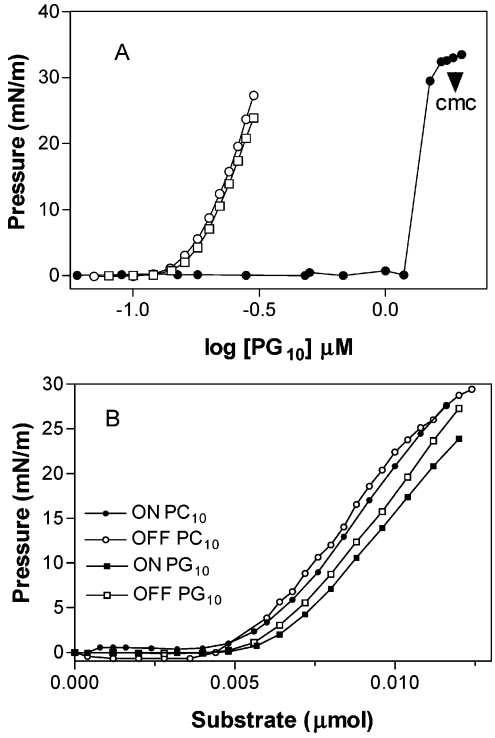

FIGURE 8: Panel A shows the dependence of equilibrated surface pressure as a function of log [PG10] μM. The lipid was added to the surface with stirring off (○) or stirring on (□) or injected into the aqueous subphase with stirring on (●). Panel B shows the change in equilibrium surface pressure by PC10 (○) or PG10 (□) amounts (in micromoles) spread on the 38.5 cm^2 surface of stirred (filled symbols) or unstirred (unfilled symbols) 40 mL of 10 mM Tris and 2 mM $CaCl_2$ at pH 8. In all four cases, a significant time-dependent drift was seen above 20 mN/m (Figure 7) that precluded measurement of the CMC. Based on these results, the onset of the compressible monolayer occurs at 0.012 μmol/40 mL = 0.3 μM phospholipid.

from the aqueous phase to the monolayer can be very slow. For example, as shown in Figure 7, the surface pressure for the PG10 monolayer stabilizes rapidly and remains stable for at least 15 min at 8 mN/m (curve a) when 0.0088 μmol of PG10 is spread on the surface of the stirred aqueous phase of the single compartment trough. With 0.012 μmol of PG10 spread on the surface, the pressure rapidly reaches 27 mN/m and then slowly drifts down for more than an hour (curve b) presumably as some of the PG10 is "solubilized". Curve c shows that the maximum pressure of about 30 mN/m develops slowly with 0.05 μmol of PG10 added to 40 mL (= 1.25 μM) of subphase. Note that if some of the monolayer (at 30 min in curve c) is removed by aspiration, the half-time for the pressure recovery is about 3 min. These results clearly show that the rate of distribution of PG10 and PC10 (results not shown) between the monolayer and the subphase are strongly pressure-dependent and can be very slow. Attempts were made to measure the effect of the sweep rate and the rate of desorption and adsorption of the product on the pressure−area curves. These results (not shown) suggest a nonideal distribution and partitioning of the substrate and the products in the monolayer as well as in the subphase, which precludes quantitative analysis.

All monolayer measurements are carried out below the CMC of the lipid: the onset of micellization is believed to occur at concentrations where the surface pressure reaches its maximum (Figure 8A). As also shown in Figure 8A,B,

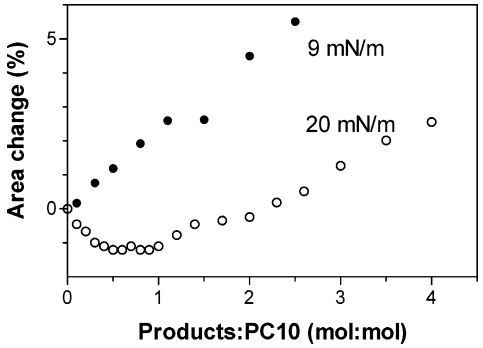

FIGURE 9: The change in the surface area of a PC10 (20 nmol) monolayer at 9 (closed symbols) or 20 mN/m (open symbols) due to the partitioning of the products of hydrolysis (LPC/FA 1:1). Typically, the solution of the products was spread on the PC10 monolayer in a stirred subphase, and the area change was allowed to equilibrate for about 10 min during which the solvent evaporates and the product equilibrates. These conditions are close to those for the zero-order reaction progress, that is, the reaction compartment is connected to a monolayer reservoir. The area expansion is monitored as the barrier displacement in the reservoir compartment. Independent controls suggested that the equilibration time for the product present in the aqueous phase is considerably longer.

partitioning of PG10 or PC10 into the air−water surface occurs only above a certain concentration of the added phospholipid. For example, a sharp increase in the surface pressure occurs above 0.2 μM PG10 spread on the (stirred or unstirred) surface, whereas the onset of the increase is at 1.2 μM PG10 added to the aqueous phase. These results imply that as much as 85% of the added PG10 in the second case does not partition into the monolayer. As compared on a linear concentration scale in Figure 8B, the onset of the increase in the surface pressure occurs only after the first 0.005 μmol of phospholipid is added to the surface. There are two possible explanations for the onset of the pressure change above a certain added phospholipid concentration. The standard explanation is that all the phospholipid is in the surface ("insoluble monolayer" assumption) and at low surface densities the monolayer does not exert any lateral pressure. According to the standard model, the onset of micellization is believed to occur only after the monolayer surface pressure reaches its maximum. A second possibility is that some phospholipid remains in the subphase. In this context, surface pressure studies show that the amount of PC10 in the subphase at equilibrium changes with the surface pressure, that is, these monolayers are "sparingly" soluble (*18*). Thus it is quite likely that the partitioning of the medium-chain phospholipid substrates and the products of PLA2-catalyzed hydrolysis changes with their total concentration as well as the surface pressure.

Pressure Dependence of the Product Partitioning. Although the products of PLA2 hydrolysis of PC10 or PG10 do not form a compressible monolayer by themselves, they partition into a substrate monolayer, as deduced from the expanded compression isotherms compared to the pure lipid (*17*). As shown in Figure 9, at two different surface pressures the area of PC10 monolayer at equilibrium changes significantly with the added products. The area change is an indirect measure of the equilibrium partitioning of the products in the PC10 monolayer under the kinetically relevant conditions of zero-order reaction progress. Also note that the partitioning behavior appears ideal at 9 mN/m as the area increases linearly with the added product concentration. On the other

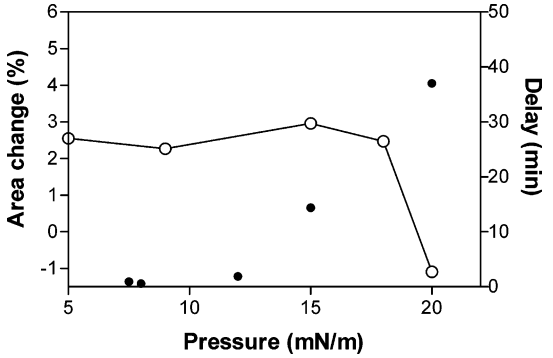

FIGURE 10: The percent change in the area (○) as a function of the surface pressure of a PC10 monolayer equilibrated with an equimolar amount of the products spread in the reaction compartment and surface pressure dependence of the delay to the steady state (●) for the hydrolysis of PC10 monolayer by 10.6 μg PLA2. The magnitude of the delay (<5 min) below 10 mN/m does not depend on the enzyme concentration (not shown; however, see Figure 3). Longer delays of >5 min observed above 10 mN/m depend on the PLA2 concentration (also see Figure 3).

hand, considerable nonideality is apparent at 20 mN/m where, after an initial decrease, a linear area expansion is observed only after an equimolar amount of the product has been added.

Based on these results, additional assumptions about miscibility and complex formation in the monolayer are required for the calculation of X_P* for the inhibition of E*. It is not possible to do so because the pressure dependence of the area expansion by added product shows a complex behavior. As summarized in Figure 10, the percent increase in the area of 20 nmol of PC10 monolayer induced by 20 nmol of products shows a complex dependence on the surface pressure. Below 18 mN/m, the area increase is relatively constant at 2−3%. At the higher surface pressures, the product-induced area expansion decreases sharply, as if partitioning of the product in the PC10 monolayer is lower or the product forms a molecular complex with nonadditive surface area. As shown in Figure 10, the onset of the long delay also occurs at surface pressures above 12 mN/m. Together these results suggest that a nonideality in the partitioning or mixing of the product in PC10 monolayer is at least in part responsible for the onset of the long delay.

Simulation of the Short Delay due to Stationary Diffusion of E Through the Unstirred Layer. The short delay of about 1 min is observed with PG10 monolayers at all pressures and with the PC10 monolayer at the lower surface pressure. The enzyme initially added to the stirred aqueous subphase (Figure 1) has to bind to the monolayer before catalysis can start. This association step will lead to a short delay that can be modeled as follows. [M*] denotes the concentration of lipid present in the monolayer, k_{on} and k_{off} are the rates of enzyme binding and dissociation, and $K_d = k_{off}/k_{on}$ is the dissociation constant. If there are no problems with surface coverage, the fraction of enzyme bound at the monolayer at equilibrium will be $F_E^{bound} = [M^*]/([M^*] + K_d)$. The equilibration time for binding is $1/(k_{on}[M^*] + k_{off})$. This will also correspond to a time delay before steady-state catalytic turnover can take place. Thus,

$$\tau_E = \frac{1}{k_{on}[M^*]} F_E^{bound} = \frac{Ld}{D_E} F_E^{bound} \qquad (1)$$

The last equality is if the binding is limited by the diffusion through the unstirred layer of width d (*2*, *12*). If $d = 10^{-3}$ cm, the depth of the trough $L = 1$ cm, the diffusion constant of the enzyme $D_E = 10^{-6}$ cm^2 s^{-1}, and $F_E^{bound} = 0.05$, the delay will be about 1 min. According to this model, the duration of the short delay is consistent with the equilibration time by stationary diffusion of PLA2 from the stirred subphase to the monolayer through the unstirred aqueous layer. In keeping with eq 1, the delay depends on the thickness of the unstirred layer, the trough geometry (Figure 1), and the equilibrium binding strength. Figure 5A suggests that the maximal rate depends on surface pressure. Figure 5B suggests that at high enzyme concentration, the maximal rate saturates. In the model, this can be understood if product desorption becomes limiting at high enzyme concentration or if the monolayer surface saturates with bound enzyme.

Also note that the unstirred-layer effects for suspended particles such as vesicles and micelles are not significant because this effect is incorporated in the $4\pi DR$ factor of diffusion-limited association, which corresponds to a stationary diffusion flux across a depleted layer of thickness roughly equal to the interaction radius R. We should also stress that the delay comes from a slow association rate, which does not by itself require an unstirred layer. It could equally well be that the enzyme does not stick very easily; then the unstirred layer becomes irrelevant.

Simulation of the Product-Dependent Long Delays. In analogy with the delays observed with phosphatidylcholine vesicles (*2*, *32*), we believe that the enzyme is not fully active on the zwitterionic interface. Full activity would not be reached until a sufficient amount of product, and thereby anionic charge, had accumulated in the interface. If product has a finite desorption rate from the interface, a steady state will be reached when the product desorption equals the rate of product formation by the activated enzyme. As we have shown before (*2*), the long time delays can be generated by activation in a variety of ways. For the simulation of the reaction progress in Figure 11, we relied on values of the kinetic parameters from the bilayer studies and assumed a linear dependence of the k_{cat}* activation on the product concentration in the monolayer. Based on such simulations, it appears that the partitioning and possibly the distribution of the products in PC10 monolayer changes at the higher pressures; this is also consistent with the results in Figure 10. If we assume that the onset of the steady state occurs when a critical density of the anionic charge develops in the interface, then a pressure-dependent decrease in the partitioning of the product will increase the delay to the steady state. Unfortunately, such processes cannot be quantified because we do not have a good way of knowing the surface pressure dependence of X_P* and the rate of product desorption from the monolayer interface. In Figure 11, we show the simulation for the enzyme-concentration dependence of the reaction progress at constant pressure assuming a constant product desorption rate and k_{cat}* activation. The parameter values as given in the caption were chosen such that the simulations would mimic the experimental results in Figures 2 and 3.

DISCUSSION

Results in this paper show that the long delay to the onset of the steady-state phase of the reaction progress for the

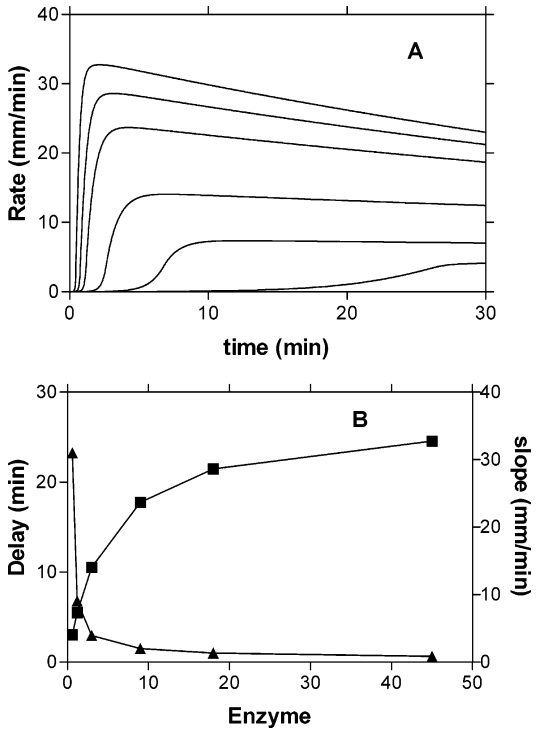

FIGURE 11: Simulated reaction progress assuming a 1000-fold k_{cat}* activation above X_P* = 0.1, a constant product desorption rate k_{diss} = 0.012 s^{-1}, and partitioning such that 2% of the product would be present in the monolayer at equilibrium. k_{cat}* is assumed to increase linearly with X_P* until it reaches a maximum at X_P* = 0.1, after which it remains constant at a 1000-fold higher level. Enzyme binding rate is 0.02 s^{-1}, that is, 50 s equilibration time (eq 1). Panel A shows the rate versus time at different enzyme amounts and panel B the maximum rate (■, right scale) and time delay (▲, left scale) versus enzyme amount (arbitrary scale). Data points correspond to the curves simulated in panel A. The scale for the enzyme concentration on the *x*-axis depends on k_{cat}*(max), K_m*, and how large a fraction of the total amount of enzyme is bound at equilibrium (none of which is known). The amount of bound E is assumed to be proportional to the total amount of E added.

hydrolysis of PC10 monolayer (Figure 3A) decreases both with increasing enzyme amounts and with decreasing pressure. The long delay is considerably reduced when products are added to the monolayer before initiating the reaction (Figure 6B). All of these observations suggest that the long delay is associated with a slow buildup of the product in the monolayer under the zero-order conditions at constant pressure. It may be emphasized here that the partitioning of the product in the substrate monolayer has been ignored in virtually all published interpretations (*3*−*15*) of the enzyme kinetic behavior on monolayers.

Accumulation of the PLA2 products in the substrate monolayer leads to an increasing negative charge that can activate the enzyme by increasing its binding (E*) or its catalytic rate (k_{cat}*). This notion that activation is induced by negative charge on the interface is also supported by the observation that there is no long delay with the anionic substrate (PG10) and that the delay in PC10 monolayers is considerably reduced when there is a high salt concentration (4 M NaCl) in the subphase, which generates an anionic interface. These results are in accord with the results obtained under the first-order conditions at constant area of monolayer (*17*) and also with those with bilayers and micelles of phosphatidylcholines (*1*, *2*, *16*, *24*−*32*). A key feature of the monolayer reaction progress is also observed with the bilayer vesicles: A long delay occurs with zwitterionic phophatidylcholine interfaces but not with the anionic interfaces including the product-containing phosphatidylcholine interface (*24*−*32*). Together these results leave little doubt that the partitioning and distribution of the products precede the onset of the steady state in the reaction progress. As shown in this paper, additional factors that depend on the trough geometry are also responsible for the short delay in the monolayer reaction progress. The challenge of establishing the turnover path and the microscopic variables for the enzyme, substrate, and the product concentrations (mole fractions) in the monolayer is particularly difficult.

Contrary to the common assumption (*3*−*15*), a significant amount of the product remains in the monolayer during the steady state and also at equilibrium. Based on the sum total of the evidence at all the interfaces, the product accumulation in the PC10 monolayer is expected to have three different effects: first, a shift in the E to E* equilibrium for PLA2; second, the anionic charge promotes interfacial k^*_{cat} activation of E*; third, the product in the interface is a competitive inhibitor as well as a surface diluent such that $X_P^* + X_S^* = 1$. In the simplest picture, it can be assumed that the turnover path for the monolayer reaction progress is interfacial and that the underlying rate and equilibrium parameters for monolayers are likely to be comparable to those for vesicles and micelles. Additional assumptions about the distribution of the products in the monolayer are necessary to describe the reaction progress. For example, the barrier displacement as a measure of the zero-order reaction progress shows that at least some of the product is desorbed in the aqueous phase, but we have not been able to measure exactly what fraction is desorbed and at what rate. A steady-state level of the product would build up in the monolayer if the desorption of the product is not instantaneous after its formation. Even if the product is instantaneously desorbed, X_P* in the monolayer would increase as the product accumulated in the aqueous phase partitions (equilibrates) into the substrate monolayer.

Characteristics of PC10 monolayers with the products of PLA2-catalyzed hydrolysis provide independent support for the view that the phase behavior of such a ternary interface shows nonideal partitioning and distribution characteristics at the higher surface pressure (Figure 9). The origin of the nonideal behavior of the product distribution as a function of surface pressure in the PC10 monolayer is not clear. Without knowing the partition behavior, area effects, and desorption rates of the product, it is impossible to infer the primary catalytic rates of the enzyme from the observed rate of area change in the monolayer assay.

The results and analysis essentially discredit the use of monolayer kinetics for the study of interfacial turnover and activation. The turnover parameters cannot be determined because an unequivocal kinetic path cannot be assigned. As an integral part of the monolayer trough geometry, the delays of a few minutes have little to do with any of the rate processes that can be characterized as the "activation" of PLA2 at the monolayer interface. In fact, interpretation of the delay as a measure of the penetrating power had become suspect ever since it became clear that such delays are not seen with micellar and bilayer substrates. To the best of our knowledge, a slow kinetic activation of an interfacial enzyme

in the pre-steady-state phase has not been shown for any interfacial enzyme.

REFERENCES

1. Berg, O. G., Gelb, M. H., Tsai, M. D., and Jain, M. K. (2001) Interfacial enzymology: The secreted phospholipase A_2-paradigm, *Chem. Rev. 101*, 2613−2653.
2. Berg, O. G., and Jain, M. K. (2001) *Interfacial Enzyme Kinetics*, John Wiley & Sons, Ltd, England.
3. Ransac, S., Ivanova, M., Verger, R., and Panaiotov, I. (1997) Monolayer techniques for studying lipase kinetics, *Methods Enzymol. 286*, 263−292.
4. Zographi, G., Verger, R., and De Haas, G. H. (1971) Kinetic analysis of the hydrolysis of lecithin monolayers by phospholipase A_2, *Chem. Phys. Lipids 7*, 185−206.
5. Verger, R., Mieras, M. C. E., and DeHaas, G. H. (1973) Action of phospholipase A at interfaces, *J. Biol. Chem. 248*, 4023−4034.
6. Verger, R., and DeHaas, G. H. (1976) Interfacial enzyme kinetics of lipolysis, *Annu. Rev. Biophys. Bioeng. 5*, 77−117.
7. Panaiotov, I., Ivanova, M., and Verger, R. (1997) Interfacial and temporal organization of enzymatic lipolysis, *Curr. Opin. Colloid Interface Sci. 2*, 517−524.
8. Pattus, F., Slotboom, A. J., and De Haas, G. H. (1979) Regulation of phospholipase A_2 activity by the lipid-water interface-Monolayer approach, *Biochemistry 18*, 2691−2697.
9. Van der Wiele, F. C., Atsma, W., Roelofsen B., Van Linde, M., Van Binsbergn, J., Radvanyi, F., Raykova, D., Slotboom, A. J., and DeHaas, G. H. (1988) Site-specific epsilon-NH_2 monoacylation of pancreatic phospholipase A_2. 2. Transformation of soluble phospholipase A_2 into a highly penetrating membrane bound form, *Biochemistry 27*, 1688−1694.
10. Verheij, H. M., Egmond, M. R., and De Haas G. H. (1981) Chemical modification of the alpha-amino group in snake venom phospholipases A_2 − A comparison of the interaction of pancreatic and venom phospholipases with lipid-water interfaces, *Biochemistry 20*, 94−99.
11. Rao, C. S., and Damodaran, S. (2002) Is interfacial activation of lipases in lipid monolayers related to thermodynamic activity of interfacial water? *Langmuir 18*, 6294−6306.
12. Fanani, M., and Maggio, B. (2000) Kinetic steps for the hydrolysis of sphingomyelin by *Bacillus cereus* sphingomyelinase in lipid monolayers, *J. Lipid. Res.* 1832−1840.
13. Yedgar, S., Cohen, R., Gatt, S., and Barenholz, Y. (1982) Hydrolysis of monomolecular layers of synthetic sphingomyelins by sphingomyelinase of *Streptococcus aurus*, *Biochem. J. 201*, 597−603.
14. Tanaka, K., Manning, P. A., and Yu, H. (2000) Lipase catalysis on monolayers at the air−water interface. 1. Kinetic rate constants on quasi-two-dimension, *Langmuir 16*, 2665−2671.
15. Tanaka, K., Mecca, S. P., and Yu, H. (2000) Lipase catalysis on monolayers at the air−water interface. 2. Diffusion-controlled kinetics in quasi-two-dimension, *Langmuir 16*, 2672−2676.
16. Jain, M. K., and Berg, O. G. (1989) The kinetics of interfacial catalysis by phospholipase A_2 and regulation of interfacial activation − Hopping versus Scooting, *Biochim. Biophys. Acta 1002*, 127−156.
17. Cajal, Y., Alsina, M. A., Berg, O. G., and Jain, M. K. (2000) Product accumulation during the lag phase as the basis for the activation of phospholipase A_2 on monolayers, *Langmuir 16*, 252−257.
18. Schwarz, G., and Zhang, J. (2001) Chain length dependence of lipid partitioning between the air/water interface and its subphase. Thermodynamic and structural implications, *Chem. Phys. Lipids 110*, 35−45.
19. Weis, R. M., and McConnell, H. M. (1984) Two-dimensional chiral crystals of phospholipid, *Nature 310*, 47−49.
20. Fischer, A., Losche, M., Mohwald, H., and Sackman, E. (1984) On the nature of the lipid monolayer phase-transition, *J. Phys. Lett. 45*, L785−791.
21. Maloney, K. M., and Grainger, D. W. (1993). Phase-separated anionic domains in ternary mixed lipid monolayers at the air−water interface, *Chem. Phys. Lipids 65*, 31−42.
22. Maloney, K. M., Grandbois, M., Grainger, D. W., Saless, C., Lewis, K. A., and Roberts, M. F. (1995) Phospholipase A_2 domain formation in hydrolyzed asymmetric phospholipid monolayers at the air/water interface, *Biochim. Biophys. Acta 1235*, 395−405.
23. Reichert, A., Ringsdorf, H., and Wagenknecht, A. (1992) Spontaneous domain formation of phospholipase A_2 at interfaces − Fluorescence microscopy of the interaction of phospholipase-A2 with mixed monolayers of licithin, lysolecithin and fatty-acid, *Biochim. Biophys. Acta 1106*, 178−188.
24. Berg, O. G., Yu, B.-Z., Rogers, J., and Jain, M. K. (1991) Interfacial catalysis by phospholipase A_2 − Determination of the interfacial kinetic rate constants, *Biochemistry 30*, 7283−7297.
25. Berg, O. G., Rogers, J., Yu, B. Z., Yao, J., Romsted, L. S., and Jain, M. K. (1997) Thermodynamic and kinetic basis of interfacial activation: Resolution of binding and allosteric effects on pancreatic phospholipase A_2 at zwitterionic interfaces, *Biochemistry 36*, 14512−14530.
26. Jain, M. K., Gelb, M. H., Rogers, J., and Berg, O. G. (1995) Kinetic basis for interfacial catalysis by phospholipase A_2, *Methods Enzymol. 249*, 567−614.
27. Apitz-Castro, R. J., Jain, M. K., and De Haas, G. H. (1982) Origin of the latency phase during the action of phospholipase A_2 on unmodified phosphatidylcholine vesicles, *Biochim. Biophys. Acta 688*, 349−356.
28. Jain, M. K., Egmond, M. R., Verheij, H. M., Apitz-Castro, R. C., Dijkman, R., and De Haas, G. H. (1982) Interaction of phospholipase A_2 and phospholipid bilayers, *Biochim. Biophys. Acta 688*, 341−348.
29. Ramirez, F., and Jain, M. K. (1991) Phospholipase A_2 at the bilayer interface, *Proteins 9*, 229−239.
30. Jain, M. K., and Rogers, J. (1989) Substrate-specificity for interfacial catalysis by phospholipase A_2 in the scooting mode, *Biochim. Biophys. Acta 1003*, 91−97.
31. Rogers, J., Yu, B. Z., Serves, S. V., Tsivgoulis, G. M., Sotiropoulos, D. N., Ioannou, P. V., and Jain, M. K. (1996) Kinetic basis for the substrate specificity during hydrolysis of phospholipids by secreted phospholipase A_2, *Biochemistry 35*, 9375−9384.
32. Upreti, G. C., and Jain, M. K. (1980) Action of phospholipase A_2 on unmodified bilayers: organizational defects are preferred sites of action, *J. Membr. Biol. 55*, 113−123.

BI049816T